Asian Journal of Chemistry; Vol. 37, No. 5 (2025), 1169-1175

ASIAN JOURNAL OF CHEMISTRY

https://doi.org/10.14233/ajchem.2025.33606

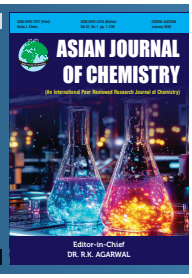

Green Synthesis, Characterization and Antioxidant Activities of Cobalt Oxide Nanoparticles Synthesized by *Ficus religiosa* Leaf Extract

R. Priyanka[1], L. Lakshmi[1,*], M. Padma[2], V. Anbarasan[3] and K. Arivalagan[4]

[1]Department of Chemistry, Dr. Ambedkar Government Arts College, Chennai-600039, India
[2]Department of Chemistry, Bharathi Women's College, Chennai-600108, India
[3]Department of Chemistry, DMI College of Engineering, Chennai-600123, India
[4]Department of Chemistry, Government Arts College for Men(A), Chennai-600035, India

*Corresponding author: E-mail: lakshmi251979@gmail.com

Received: 3 March 2025; *Accepted*: 9 April 2025; *Published online*: 30 April 2025; AJC-21984

In present investigation, *Ficus religiosa* leaf extract, as a reducing agent, was effectively used to synthesize cobalt oxide nanoparticles using a rapid, low-cost and eco-friendly approach. The green fabricated cobalt oxide nanoparticles were confirmed by microscopic and spectroscopic analytical technique such as ultra violet-visible (UV-Vis), Fourier transforms infrared (FTIR), X-ray diffraction (XRD), dynamic light scattering (DLS) and zeta potential measurements. The surface area covered by the nanoparticles has been calculated using BET analysis, scanning electron microscopy (SEM), energy dispersive X-ray spectroscopy (EDS) and transmission electron microscopy (TEM). The antioxidant activity of cobalt oxide nanoparticles was evaluated, revealing their effectiveness and indicating potential applications.

Keywords: Green synthesis, Cobalt oxide nanoparticles, *Ficus religiosa* leaves extract, Antioxidant activity, DPPH and FRAP.

INTRODUCTION

The synthesis of nanoparticles employs numerous approaches that are extensively documented in the literature [1,2]. The use of harmful reducing and capping agents is inherent in the physical and chemical methods used for producing nanoparticles of uniform size [3,4]. Plant mediated green synthesis of metal oxide nanoparticles has attracted scientists and researchers from harmful methods, due to their benign, non-toxic nature and eco-friendliness [5,6]. Plant-based nanoparticles, synthesized from different sources, have found major application in targeted drug delivery and treatment of cancerous cells [7-9]. As plants consist of different types of phenolic compounds and are responsible for the redox reaction and results in the successful production of nanoparticles [10,11]. Various phytochemicals in plants function as capping, stabilizing and reducing agents, minimizing the agglomeration of nanoparticles and conferring unique characteristics that regulate structural morphology and stabilize the nanoparticle formation process [12]. Plant-based nanoparticles possess several advantages, such as their wide availability, safety and variety of biomolecular compounds, which are the components that facilitate nanoparticle synthesis [13,14].

Being relatively cheap non-precious metal oxide and demonstrating catalytic properties similar to platinum and palladium, cobalt oxide has attracted research interest till date. P-type semiconductor Co_3O_4 NPs are the transition metal oxides that exhibit many oxidation states, including Co^{2+}, Co^{3+} and Co^{4+} [15]. Its spinel structure makes Co_3O_4 NPs the most stable among a variety of structures and are the promising candidate for a large variety of applications in lithium-ion batteries, gas sensors, supercapacitors, drug delivery agents, antimicrobial agents and purification and photocatalysis [16-19]. Furthermore, the Co_3O_4 NPs have been found to be economically viable in comparison to other noble metals [20]. Cobalt oxide nanoparticles as therapeutic agents have been investigated in treating diseases related to microbial infections, making them interesting candidates for use in biomedical applications [21]. Compared to the antibiotics, Co_3O_4 NPs had lesser side effects, a higher concentration antibacterial, antifungal and antioxidant properties and are non-toxic to the human body [22].

Based on the literature survey, the green synthesis of cobalt oxide nanoparticles using various plant extracts were reported including the leaf extracts of *Aspalathus linearis* [23], *Helianthus annuus* [24], peel extracts of *Punica granatum* [25] and fruit extracts of *Terminalia chebula* [26]. However, there is no report about the synthesis, characterization of cobalt oxide nanoparticles using *Ficus religiosa* leaves extract as a stabilizing and reducing agent and also evaluated its antioxidant activity.

EXPERIMENTAL

The analytical grade chemicals and solvents used for the synthesis of cobalt oxide nanoparticles were obtained and therefore, not conducted to any further purification. Chemicals were procured from Kevin Laboratories, Chennai, analytical grade cobalt nitrate hexahydrate ($Co(NO_3)_2{\cdot}6H_2O$, 98% purity), hydrochloric acid and sodium hydroxide.

Preparation of *Ficus religiosa* leaf extract: The fresh matured leaves of *F. religiosa* were collected from the local garden and washed thoroughly under running tap water and then rinsed several times with double distilled water. The washed leaves were cut into small pieces, air-dried for 5 to 10 days in a shade and ground to a coarse powder using an electric blender. The dried powder was stored in an air-tight container until use again. A 10 g sample of leaf powder was mixed with 250 mL of double distilled water, heated on a water bath for 30 min at 80 and 90 ºC and cooled for 1 h. The supernatant was filtered using Whatman No. 1 filter paper to remove any foreign material and then centrifuged at 1200 rpm for 15 min. The resulting pale brown solution was adjusted to pH 11 with 0.1 NaOH solution and preserve for further use [27].

Synthesis of cobalt oxide nanoparticles: A freshly prepared solution of $Co(NO_3)_2{\cdot}6H_2O$ (0.1 M) was added wth *Ficus religiosa* leaf extract dropwise in a 5:5 ratio for 30 min period. As a cloud of particles appeared, a clear change of colour in the solution indicated the presence of nanostructures formation. The solution was further centrifuged and the residue so obtained was dried in a hot-air oven for 24 h at 100 ºC. Synthesized cobalt oxide nanoparticles were kept in the muffle furnace at 350 ºC for 4 h. Freshly synthesized cobalt oxide nanoparticles thus kept in Amber vials and stored in air-tight containers were ready for further characterization [28].

Characterization: The green synthesized cobalt oxide nanoparticles was characterized by UV-visible spectroscopy using Elico SL210 instrument in the spectral range of 200–400 nm; FT-IR (Shimadzu-8400S spectrophotometer) spectra was obtained using KBr method in the range of 4000-400 cm^{-1}. The XRD analysis was conducted with Bruker D8 Advance, X-ray powder diffractometer and the data were recorded in the range of 2θ values from 10 to 90º with a scanning rate of 4º min^{-1} by using the Cu-*K*α radiation with a λ_{max} of 1.54 Å. The BET technique was used to dentify the pore diameter, specific surface area, pore volume, and size distributiom with the help of Micromeritics instrument (model ASAP2020 Porosimeter). The morphological analysis for the surface was done by SEM (JOEL-6390LA) and TEM (JEOL JEM2100 HR-TEM) techniques. The DLS was carried out using Spectro scatter-201 instrument in DMSO medium.

RESULTS AND DISCUSSION

UV-visible absorption studies: The UV-Vis spectra of *F. religiosa* leaf extract and the green synthesized CoO NPs are shown in Fig. 1. The absorption maximum observed at 234 nm in the extract-theoretical spectrum has shifted to 301 nm, indicating that the phytocompounds present in the extract reduced the cobalt ions into CoO NPs efficiently. The small peak observed may be responsible for tiny organic molecules in the reaction mixture. The UV data may support the characterization of plant extract mediated cobalt oxide nanoparticles [29].

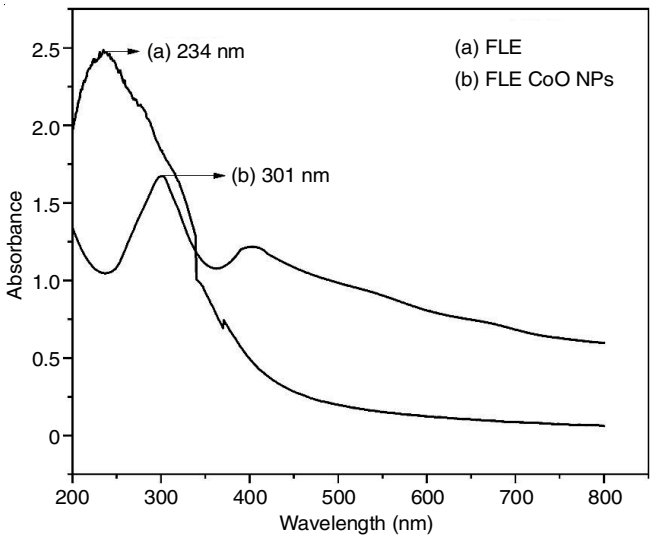

Fig. 1. UV-visible absorbance spectra of *Ficus religiosa* leaf extract and CoO NPs

By utilizing the Planck's equation, the band energy gap of CoO NPs from UV-Vis spectrum was calculated using the following eqn. 1:

$$E_{bg} = \frac{1240}{\lambda}(eV) \quad (1)$$

where λ is the absorption maximum wavelength (301 nm) and the E_g value of CoO NPs was found to be 4.12 eV [30].

FT-IR analysis: The FTIR spectrum of *F. religiosa* leaf extract show peaks at the wavelength of 3329, 2215 and 1620 cm^{-1} (Fig. 2a). A peak at 3329 cm^{-1} is due to the stretching vibration of amino and hydroxyl groups (-NH and -OH). The band in the region of 2215 cm^{-1} is assigned to the stretching vibration of C-H bands due to the presence of $-CH_2-CH_3$ groups in the structure of leaf extract. The shouldered peak appeared at 1620 cm^{-1} is due to the stretching vibrations of carbonyl compounds, which indicates the presence of fatty acids present in the leaf extract.

In the FTIR spectrum of cobalt oxide nanoparticles (Fig. 2b), the broad peak at 3316 cm^{-1} with decreased transmittance observed because the cobalt metal ions reduce the various -OH groups present in the alcohols. Similarly, the -C-H stretching vibration of alkyl deformation also reduced by cobalt ions. Peak at 2021 cm^{-1} denotes the C-H stretching of the H-bonded alkane, whereas the peaks cantered at 1618 cm^{-1} is due to stretching and bending vibration of -OH group of the water

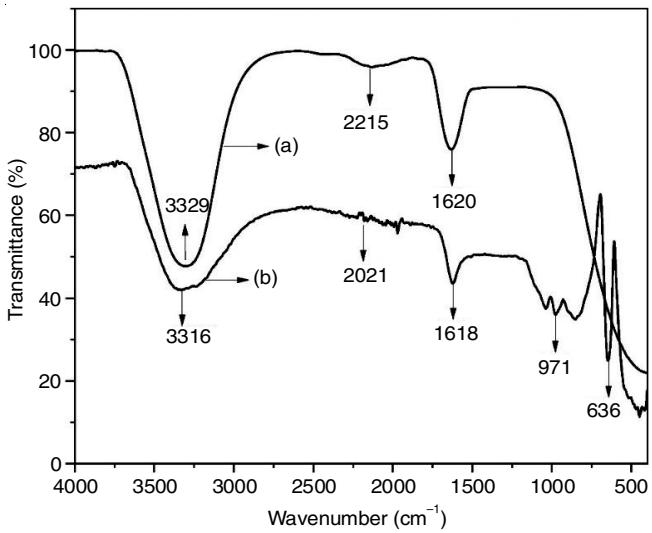

Fig. 2. FT-IR spectra of (a) *Ficus religiosa* leaf extract and (b) cobalt oxide nanoparticles

molecules. The peak at 971 cm^{-1} is due to the stretching vibration of NO_3^-, which may be due to the adherence of cobalt nitrate salt, which was used as precursor material for the synthesis procedure. The observed peak at 636 cm^{-1} is represented with Co-O and O-Co-O stretching frequency confirmed the configuration of cobalt oxide nanoparticles [31].

Structural analysis: The XRD pattern of biogenic CoO NPs manifests a clear monoclinic structure whose characteristic 2θ are 19.02º, 31.32º, 36.79º, 44.90º, 59.42º and 65.37º, respectively with respect to the planes (111), (220), (311), (222), (511) and (440) (Fig. 3). All the diffraction peaks are matched with the JCPDS card no. 073-1701 [32,33]. From the XRD results, the diffraction peaks of synthesized CoO NPs along with other unknown impurities were also observed and therefore their crystallite values seem to be lower. The crystallite size of the CoO NPs was calculated by using the Debye-Scherrer's equation [34]:

$$D = \frac{k\lambda}{\beta \cos\theta} \quad (2)$$

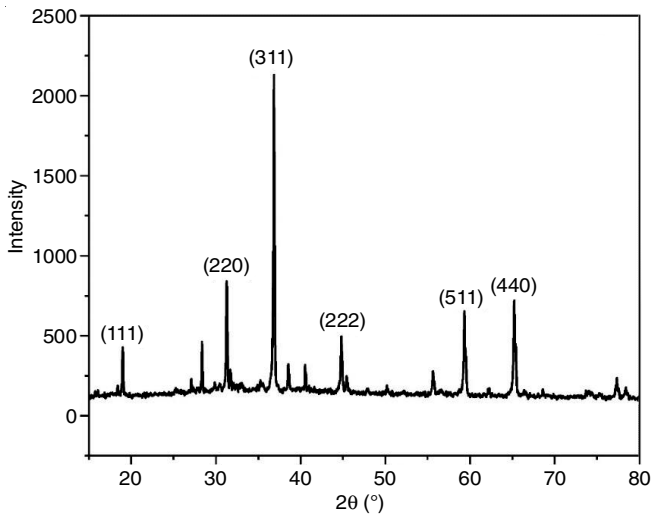

Fig. 3. X-ray diffraction spectrum of cobalt oxide nanoparticles

where D represents the crystallite size; k represents the instrument constant 0.89 for spherical nanoparticles; θ is the diffraction angle; β denotes full width at half maximum (FWHM) and λ is the wavelength of the X-ray radiation (0.154 nm).

The average crystallite size of cobalt oxide nanoparticles was found to be 35 nm. The highest diffraction peak assigned to 311 crystal planes is about 36.79º positions. X-ray diffraction analysis shows a number of peaks between 19.02 and 65.37º, while the maximum intensity is located at 36.79º [35]. The value of 'd' (the interplanar spacing between the atoms) was calculated using Bragg's equation:

$$n\lambda = 2d \sin\theta \quad (3)$$

where λ is the 1.54 Å wavelength of X-rays; n denotes order of diffraction (n = 1); d represents distance between adjacent CoO layers and θ is a diffraction angel. The calculated results are depicted in Table-1.

TABLE-1
STRUCTURAL PARAMETERS OF THE BIOSYNTHESIZED COBALT OXIDE NANOPARTICLES

2θ	θ	d-spacing	FWHM	Crystallite size (D, nm)	D (nm) (average)
19.02	9.51	4.6623	0.1293	62.3068	34.97
31.32	15.66	2.8537	0.1885	43.7625	
36.79	18.40	2.4404	0.3541	23.6424	
44.90	22.45	2.0171	0.3096	27.7673	
59.42	29.71	1.5542	0.3075	29.7485	
65.37	32.69	1.4262	0.4174	22.6154	

Dynamic light scattering (DLS) and zeta potential: The particle size distribution analysis of CoO NPs synthesized with *F. religiosa* leaf extract was determined by dynamic light scattering method. The average particle size distribution for synthesized CoO NPs was in the range of 400-640 nm (Fig. 4) and larger than that measured using SEM. The larger particle sizes obtained may be attributed to nanoparticle aggregation and the formation of a hydrodynamic shell, as evidenced from previous studies [36]. This could be due to excess leaf extract used for the reduction of cobalt nitrate, corresponding to a faster rate of nucleation and growth of nanoparticles, leading to some of the particles forming smaller agglomerates. The graphs depicted in Fig. 4, concluded that a majority of particles formed were in the nanorange [37].

Zeta sizer and zeta potential spectra for dynamic light scattering will be used to check the size and potential of cobalt oxide nanoparticles in the prepared solution. The stable colloids produced had zeta potentials in the range of 16.9 mV (Fig. 5). The zeta potential distribution of CoO NPs with a good value refers to the high stability of the solution [38].

BET surface area studies: Fig. 6 illustrates that the BET analysis reveals the produced CoO nanoparticles possess a BET surface area of 2.9106 m^2/g. This findings suggest that the spherical particles are indeed large in surface area and measured in nanometres [39].

Morphological studies: The SEM morphology of CoO nanoparticles from their external appearance shows irregular, random and cubo-hexagonal shapes with various degrees of

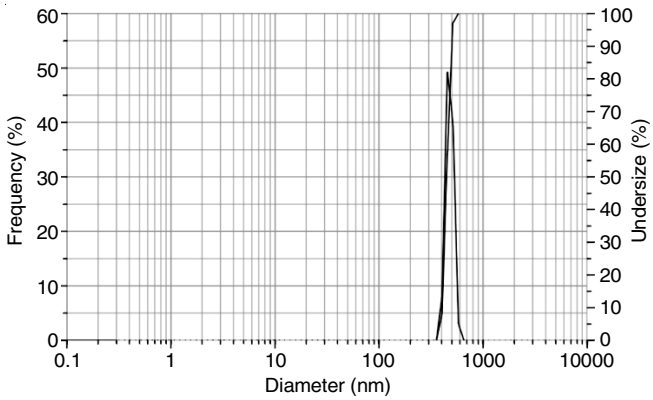

Fig. 4. DLS plot for green synthesized cobalt oxide nanoparticles

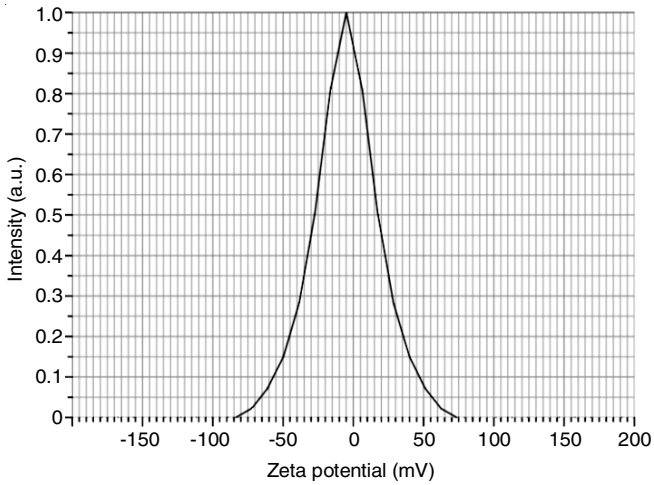

Fig. 5. Zeta potential measurement for green synthesized cobalt oxide nanoparticles

openness or agglomeration at the magnifications of 2 µm (Fig. 7a). The distribution of sizes for the average and particles was determined from Gaussian fitting of the size distribution histogram, as shown in Fig. 7d. The biogenic synthesized CoO nanoparticle sizes was ranged from 60 to 160 nm in diameter and their average diameter was found to be 120 nm. Interacting nanoparticles with large surface area and high surface energy result in agglomeration [40].

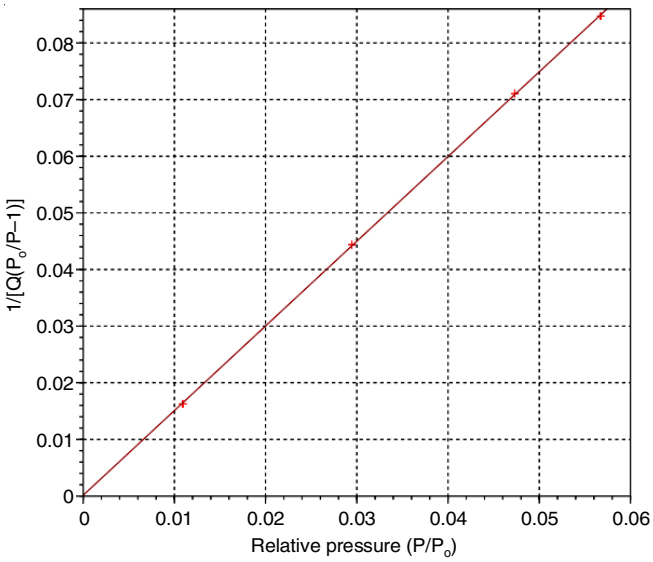

Fig. 6. BET plot of the nitrogen adsorption on the green synthesized cobalt oxide nanoparticles

The EDX spectrum showed the development of intense peaks of Co in the prepared nanoparticles (Fig. 8), which were observed between 2-3 KeV and 6.5-7.5 KeV. From the weight and atomic percentages, the elemental composition of biosynthesized CoO nanoparticles indicates that cobalt is the major element, comprising 84.52 wt.% and 59.71 at.%. Cobalt oxide nanoparticles contained oxygen, which had a weight percentage of 15.48% and atomic percentage of 40.29%. The generated biosynthesized CoO nanoparticles are in their high purity form and coincided with the earlier studies too [41].

HR-TEM-SAED analysis: The HR-TEM images of CoO nanoparticles obtained with the SAED pattern from HR-TEM studies are shown in Fig. 9a-d. The porous nanomaterials have random distributions of particle sizes ranging from 160 to 300 nm, have irregular shapes and show poorly aggregated crystalline features [42]. HR-TEM image (Fig. 9b) shows the visible lattice fringes and the interspacing was found to be 0.21 nm. The particle size distribution in average sizes was calculated using the Gaussian fitting of size histogram distribution (Fig.

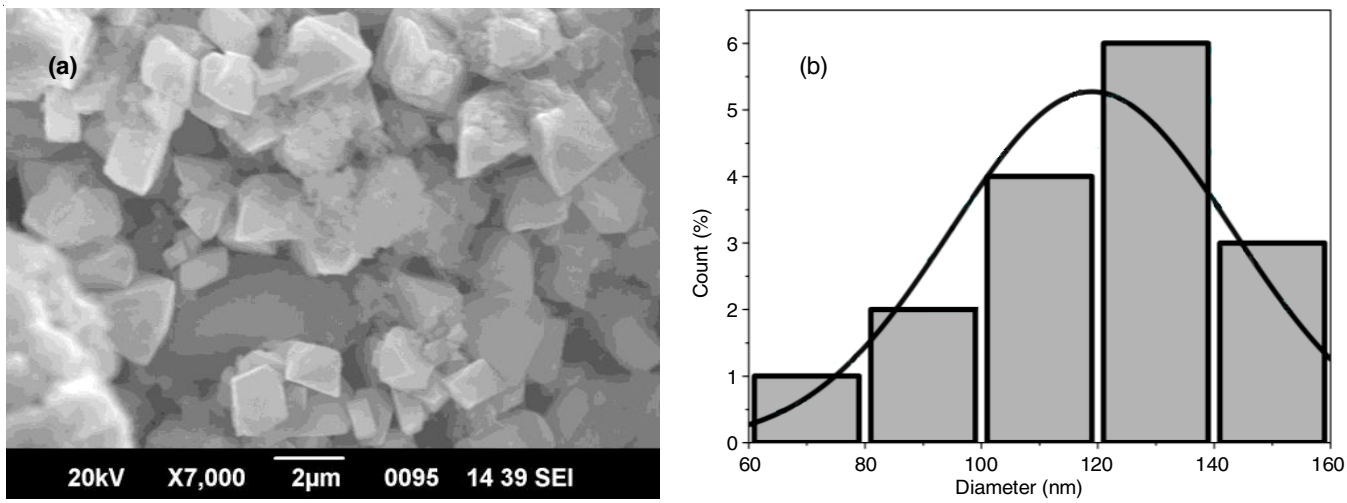

Fig. 7. SEM images of green synthesized cobalt oxide nanoparticles (a) and particle size histogram (b)

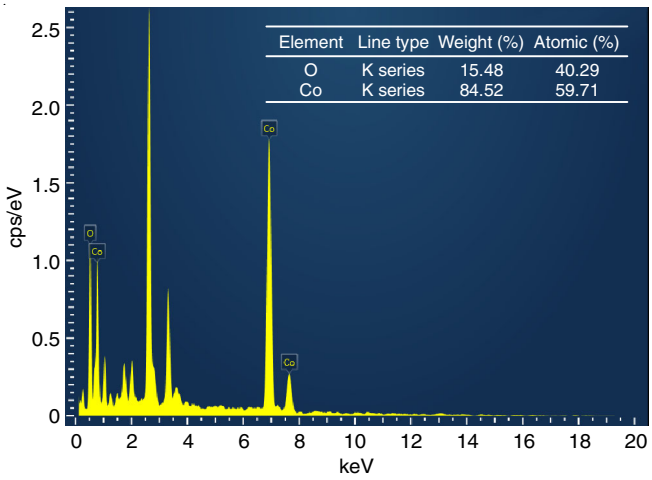

Fig. 8. EDX spectrum of cobalt oxide nanoparticles

9d). The range of particle sizes for biogenic synthesized CoO nanoparticles was between 160-360 nm, with an average particle size of 220 nm.

The SAED patterns (Fig. 9c) consist of well-defined rings, which could be indexed with a face-centered cubic cobalt phase. This finding has also been substantiated by the X-ray diffraction, which further agrees well with the EDAX spectra showing peaks corresponding to cobalt and oxygen. There is growing evidence to reflect the formation of polycrystals with well-defined diffraction spots from the SAED pattern. This observation is similar to previous report [43].

Antioxidant activities: The antioxidant activity of green synthesized cobalt oxide nanoparticle was determined by using DPPH (2,2-diphenyl-1-picrylhydrazyl) free radical assay and FRAP (ferric ion reducing antioxidant power) assay.

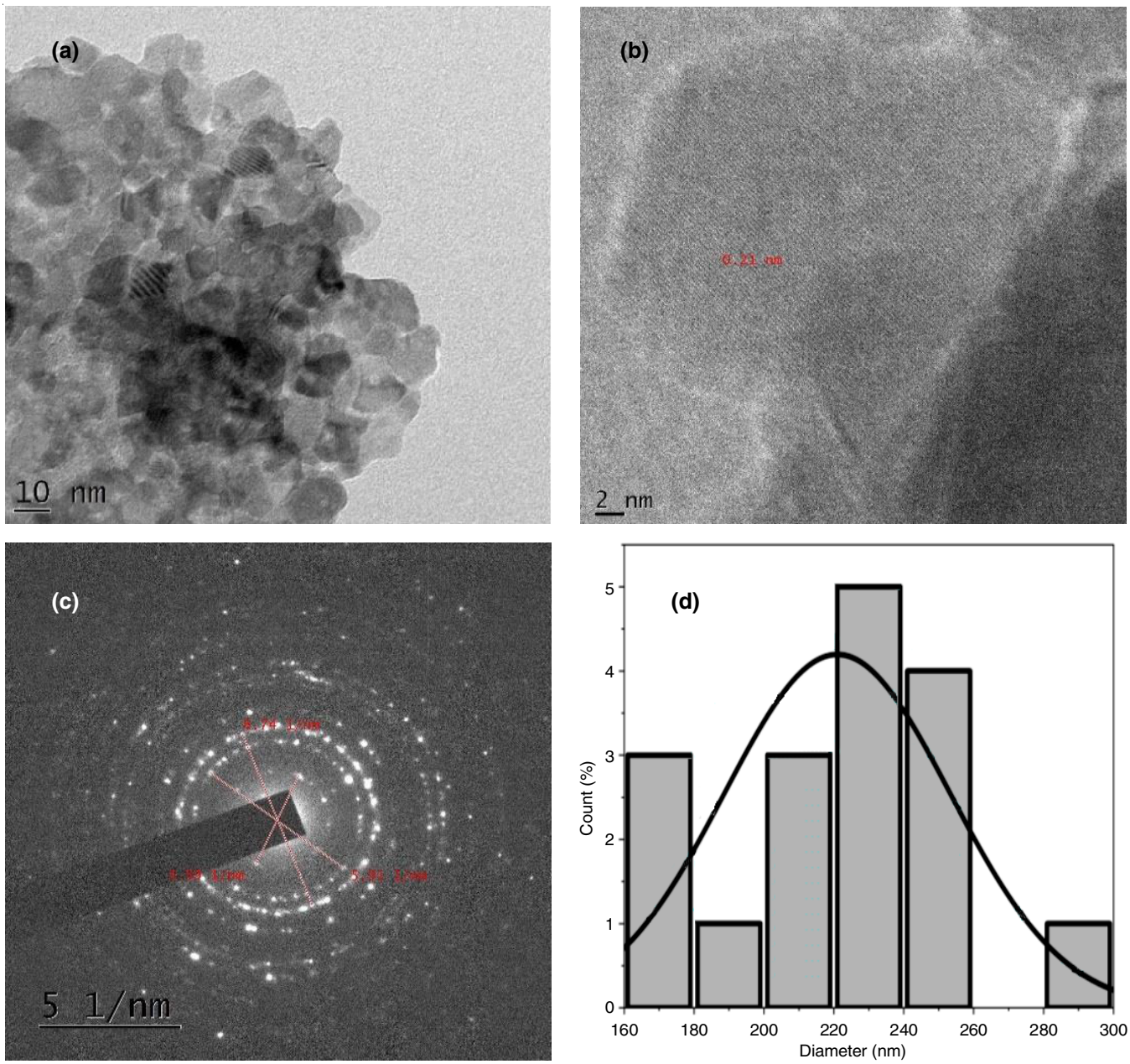

Fig. 9. (a) TEM image, (b) HRTEM image, (c) SAED pattern and (d) particle size histogram of green synthesized cobalt oxide nanoparticles

DPPH radical scavenging assay: The effect of different concentrations of CoO nanoparticles on DPPH radical antioxidant is shown in Table-2. The DPPH activity of the cobalt oxide nanoparticles was found to increase in a dose-dependent manner. At concentrations 0.4 to 2.0 mg/mL, CoO nanoparticles showed a scavenging activity ranging from 10% to 38% with average IC_{50} value, 2.735 mg/mL.

TABLE-2
DPPH RADICAL ACTIVITY

Concentration of CoO NPs	Average OD value	Activity (%)
0.4 mg/mL	1.69	10.0592
0.8 mg/mL	1.52	16.5681
1.2 mg/mL	1.49	20.7101
1.6 mg/mL	1.43	29.5858
2.0 mg/mL	1.30	38.4615

Ferric ion reducing antioxidant power (FRAP): The FRAP assay for the CoO nanoparticles was conducted at five different concentrations ranging from 0.4 g/mL to 2.0 g/mL. The FRAP assay measures the antioxidant activity by reducing Fe^{3+} ions to Fe^{2+} ions by CoO NPs at 700 nm and the results are presented in Table-3. The free radical scavenging activity of CoO nanoparticles using *F. religiosa* leaf extract was much lower when compared with the standard ascorbic acid.

TABLE-3
FERRIC ION REDUCING ANTIOXIDANT POWER OF COBALT OXIDE NANOPARTICLES

Cobalt oxide nanoparticles concentrations	Average OD value	
	Cobalt oxide nanoparticle	Standard drug ascorbic acid
0.4 mg/mL	0.14	0.77
0.8 mg/mL	0.11	0.63
1.2 mg/mL	0.08	0.42
1.6 mg/mL	0.06	0.32
2.0 mg/mL	0.04	0.26

Conclusion

A green mediated synthesis of cobalt oxide nanoparticles from *Ficus religiosa* leaf extract, where the leaf extract served as a stabilizing and reducing agent was conducted and characterized with various techniques such as UV, FTIR, XRD, DLS, BET, SEM, EDX, TEM and SAED. From the UV-Vis analysis, the surface plasmon resonance phenomenon was observed with an absorbance peak at 301 nm. The average crystallite size was estimated to be 35 nm. Appearance of single peak in DLS plot confirms the high purity of the biosynthesized cobalt oxide nanoparticles. BET analysis shows the surface area of the cobalt oxide nanoparticle is 2.9106 m^2/g. The SEM and TEM images showed the surface morphology and particles size of the cobalt oxide nanoparticles. In DPPH and FRAP assays, cobalt oxide nanoparticles concentration increased antioxidant activities also increased. The maximum and minimum radical scavenging activity of these nanoparticles is 38.5% at 2 mg/mL and 10.1% at 0.4 mg/mL.

ACKNOWLEDGEMENTS

The authors acknowledge the STIC, CUSAT, Cochin, India for conducting the electron microscopic studies. Thanks, are also due to IIT Madras, Chennai and University of Madras, Chennai, India for providing the XRD, BET and DLS analysis facilities. The authors also acknowledge the Department of Research and Development, Sree Balaji Medical College and Hospital, Chennai, India for providing the facilities of antioxidant studies.

CONFLICT OF INTEREST

The authors declare that there is no conflict of interests regarding the publication of this article.

REFERENCES

1. S. Kumari, S. Raturi, S. Kulshrestha, K. Chauhan, S. Dhingra, K. András, K. Thu, R. Khargotra and T. Singh, *J. Mater. Res. Technol.*, **27**, 1739 (2023); https://doi.org/10.1016/j.jmrt.2023.09.291
2. N. Baig, I. Kammakakam and W. Falath, *Mater. Adv.*, **2**, 1821 (2021); https://doi.org/10.1039/D0MA00807A
3. R. Javed, M. Zia, S. Naz, S.O. Aisida, N. Ain and Q. Ao, *J. Nanobiotechnol.*, **18**, 172 (2020); https://doi.org/10.1186/s12951-020-00704-4
4. A.K. Sidhu, N. Verma and P. Kaushal, *Front. Nanotechnol.*, **3**, 801620 (2022); https://doi.org/10.3389/fnano.2021.801620
5. U.O. Aigbe and O.A. Osibote, *J. Hazard. Mater. Adv.*, **13**, 100401 (2024); https://doi.org/10.1016/j.hazadv.2024.100401
6. J. Singh, T. Dutta, K.-H. Kim, M. Rawat, P. Samddar and P. Kumar, *J. Nanobiotechnol.*, **16**, 84 (2018); https://doi.org/10.1186/s12951-018-0408-4
7. P. Sarvarian, P. Samadi, E. Gholipour, K.S. Asenjan, M. Hojjat-Farsangi, R. Motavalli, F.M. Khiavi and M. Yousefi, *Immunol. Invest.*, **51**, 1039 (2022); https://doi.org/10.1080/08820139.2021.1891094
8. N.A. Hanan, H.I. Chiu, M.R. Ramachandran, W.H. Tung, N.N.M. Zain, N. Yahaya and V. Lim, *Int. J. Mol. Sci.*, **19**, 1725 (2018); https://doi.org/10.3390/ijms19061725
9. X. Cheng, Q. Xie and Y. Sun, *Front. Bioeng. Biotechnol.*, **11**, 1177151 (2023); https://doi.org/10.3389/fbioe.2023.1177151
10. V.V. Makarov, A.J. Love, O.V. Sinitsyna, S.S. Makarova, I.V. Yaminsky, M.E. Taliansky and N.O. Kalinina, *Acta Natur.*, **6**, 35 (2014).
11. S.A. Filho, M.S. dos Santos, O.A.L. dos Santos, B.P. Backx, M.-L. Soran, O. Opris, I. Lung, A. Stegarescu and M. Bououdina, *Molecules*, **28**, 3060 (2023); https://doi.org/10.3390/molecules28073060
12. Z. Villagrán, L.M. Anaya-Esparza, C.A. Velázquez-Carriles, J.M. Silva-Jara, J.M. Ruvalcaba-Gómez, E.F. Aurora-Vigo, E. Rodríguez-Lafitte, N. Rodríguez-Barajas, I. Balderas-León and F. Martínez-Esquivias, *Resources*, **13**, 70 (2024); https://doi.org/10.3390/resources13060070
13. H. Singh, M.F. Desimone, S. Pandya, S. Jasani, N. George, M. Adnan, A. Aldarhami, A.S. Bazaid and S.A. Alderhami, *Int. J. Nanomed.*, **18**, 4727 (2023); https://doi.org/10.2147/IJN.S419369
14. M.M. Abady, D.M. Mohammed, T.N. Soliman, R.A. Shalaby and F.A. Sakr, *Bull. Natl. Res. Cent.*, **49**, 24 (2025); https://doi.org/10.1186/s42269-025-01316-4
15. J. Kießling, S. Rosenfeldt and A.S. Schenk, *Nanoscale Adv.*, **5**, 3942 (2023); https://doi.org/10.1039/d3na00032j
16. F. Zhao and H. Ma, *Crystals*, **13**, 634 (2023); https://doi.org/10.3390/cryst13040634

17. A. Waris, M. Din, A. Ali, S. Afridi, A. Baset, A.U. Khan and M. Ali, *Open Life Sci.*, **16**, 14 (2021); https://doi.org/10.1515/biol-2021-0003
18. X. Hu, L. Wei, R. Chen, Q. Wu and J. Li, *ChemistrySelect*, **5**, 5268 (2020); https://doi.org/10.1002/slct.201904485
19. J.K. Sharma, P. Srivastava, G. Singh, M.S. Akhtar and S. Ameen, *Mater. Sci. Eng. B*, **193**, 181 (2015); https://doi.org/10.1016/j.mseb.2014.12.012
20. S. Iravani and R.S. Varma, *Green Chem.*, **22**, 2643 (2020); https://doi.org/10.1039/D0GC00885K
21. Kainat, M.A. Khan, F. Ali, S. Faisal, M. Rizwan, Z. Hussain, N. Zaman, Z. Afsheen, M.N. Uddin and N. Bibi, *Saudi J. Biol. Sci.*, **28**, 5157 (2021); https://doi.org/10.1016/j.sjbs.2021.05.035
22. C.T. Anuradha and P. Raji, *Appl. Phys., A Mater. Sci. Process.*, **127**, 55 (2021); https://doi.org/10.1007/s00339-020-04209-7
23. A. Diallo, A.C. Beye, T.B. Doyle, E. Park and M. Maaza, *Green Chem. Lett. Rev.*, **8**, 30 (2015); https://doi.org/10.1080/17518253.2015.1082646
24. M. Saeed, N. Akram, Atta-ul-Haq, S.A.R. Naqvi, M. Usman, M.A. Abbas, M. Adeel and A. Nisar, *Green Process Synth*, **8**, 382 (2019); https://doi.org/10.1515/gps-2019-0005
25. I. Bibi, N. Nazar, M. Iqbal, S. Kamal, H.N. Bhatti, S. Nouren, Y. Safa, K. Jilani, M. Sultan, S. Ata, F. Rehman and M. Abbas, *Adv. Powder Technol.*, **28**, 2796 (2017); https://doi.org/10.1016/j.apt.2017.08.018
26. T.N.J.I. Edison, R. Atchudan, M.G. Sethuraman and Y.R. Lee, *J. Taiwan Inst. Chem. Eng.*, **68**, 489 (2016); https://doi.org/10.1016/j.jtice.2016.09.021
27. C.A. Fernandes, N. Jesudoss M, A. Nizam, S.B.N. Krishna and V.V. Lakshmaiah, *ACS Omega*, **8**, 39315 (2023); https://doi.org/10.1021/acsomega.3c04857
28. H.J. Lee, J.Y. Song and B.S. Kim, *J. Chem. Technol. Biotechnol.*, **88**, 1971 (2013); https://doi.org/10.1002/jctb.4052
29. N.Y. Maharani, *Particul. Sci. Technol.*, **40**, 662 (2022); https://doi.org/10.1080/02726351.2021.1992057
30. A. Gouasmia, E. Zouaoui, A.A. Mekkaoui, A. Haddad and D. Bousba, *Inorg. Chem. Commun.*, **145**, 110066 (2022); https://doi.org/10.1016/j.inoche.2022.110066
31. P. Kalainila, V. Subha, R.S.E. Ravindran and S. Renganathatn, *Asian J. Pharm. Clin. Res*., **7**, 39 (2014).
32. G.M. Shah and M.A. Khan, *Leaflets*, **10**, 49 (2008).
33. N. Ahmad, S. Sharma and R. Rai, *Adv. Mater. Lett.*, **3**, 376 (2012); https://doi.org/10.5185/amlett.2012.5357
34. T. Krishnakumar, R. Jayaprakash, N. Pinna, V.N. Singh, B.R. Mehta and A.R. Phani, *Mater. Lett.*, **63**, 242 (2009); https://doi.org/10.1016/j.matlet.2008.10.008
35. C.M. Magdalane, K. Kaviyarasu, M.V. Arularasu, K. Kanimozhi and G. Ramalinga, *Surf. Interfaces*, **17**, 100369 (2019); https://doi.org/10.1016/j.surfin.2019.100369
36. M.M. Modena, B. Ruhle, T.P. Burg and S. Wuttke, *Adv. Mater.*, **31**, 1901556 (2019); https://doi.org/10.1002/adma.201901556
37. N. Gandhi, Y. Shruthi, G. Sirisha and C.R. Anusha, *Haya: Saudi J. Life Life Sci.*, **6**, 89 (2021); https://doi.org/10.36348/sjls.2021.v06i05.003
38. A.C.J. Oliveira, A.R. Araújo, P.V. Quelemes, D. Nadvorny, J.L. Soares-Sobrinho, J.R.S.A. Leite, E.C. da Silva-Filho and D.A. Silva, *Carbohydr. Polym.*, **213**, 176 (2019); https://doi.org/10.1016/j.carbpol.2019.02.033
39. P. Parab, P. Aniket and A. Pawar, *Indian J. Chem.*, **63**, 15 (2024); https://doi.org/10.56042/ijc.v63i1.304
40. A. Roy and J. Bhattacharya, *Micro & Nano Lett.*, **5**, 131 (2010); https://doi.org/10.1049/mnl.2010.0020
41. R. Govindasamy, V. Raja, S. Singh, M. Govindarasu, S. Sabura, K. Rekha, V.D. Rajeswari, S.S. Alharthi, M. Vaiyapuri, R. Sudarmani, S. Jesurani, B. Venkidasamy and M. Thiruvengadam, *Molecules*, **27**, 5646 (2022); https://doi.org/10.3390/molecules27175646
42. S.K. Jesudoss, J.J. Vijaya, K. Kaviyarasu, M. Sivachidambaram, L.J. Kennedy, P.I. Rajan, H.A. Al-Lohedan, R. Jothiramalingam and M.A. Munusamy, *Photochem. Photobiol. Sci.*, **16**, 766 (2017); https://doi.org/10.1039/c7pp00006e
43. R.K. Gupta, A.K. Sinha, B.N. Raja Sekhar, A.K. Srivastava, G. Singh and S.K. Deb, *Appl. Phys., A Mater. Sci. Process.*, **103**, 13 (2011); https://doi.org/10.1007/s00339-011-6311-6